Journal of Civil Engineering and Construction 2022;11(2):89-103
https://doi.org/10.32732/jcec.2022.11.2.89

Assessment of Key Parameters Affecting Compressive Behavior of uPVC-Confined Concrete

Nwzad Abduljabar Abdulla

College of Engineering, Salahaddin Univ., Kirkuk Rd., Erbil, Iraq
E-mail: anwzad@yahoo.com

Received: 17 December 2021; Accepted: 3 February 2022; Available online: 30 April 2022

Abstract: Experimental work was conducted to evaluate the strength capacity of uPVC filled-concrete (CFPT) stub columns under different environmental conditions. The effect of three curing conditions, open-air, water, and sealed, on the CFPT specimens was examined. The water absorption of CFPT was also determined to evaluate the confining device's performance in protecting concrete in humid environments. Test results show that the plastic tube effectively reduced the water absorption of the confined concrete by more than 80%. In order to assess the influence of key parameters on the performance of CFPT under the applied load, a database was established that covered 186 axial compression test results of CFPT specimens. A detailed discussion of the key parameters affecting the overall behavior of CFPT also presented.
Keywords: Absorption; Database; Critical parameters; Plastic tube; Compression load.

1. Introduction

In recent years, attention has turned to the potential applications of innovative materials in composite construction [1]. One such promising material that has received attention is the uPVC tube, for concrete protection in hostile environments [2,3] and lightweight residential buildings [4]. Other applications of this tubing system are: embedded in reinforced concrete columns [5] or strengthened with FRP for earthquake-resistant infrastructure construction [6]. This composite system has the capacity to exhibit considerable inelastic deformation under seismic reverse loading [7,8]. The CFPT specimens owe their enhanced deformation capacities to the very high tube tensile elongation capability; 100 to 150% [9]. Several critical parameters influence the performance of CFPT under the normal load [10]. Compression concrete members show different behavior under different environmental conditions. FRP tube-encased specimens tested under different environmental conditions developed different shrinkage behavior, affecting their transition zone and dilation response [11]. So far, no research has covered the influence of concrete curing conditions on CFPT during the construction period. This was achieved by curing specimens in air, water, or sealed in a chamber. Another objective of the present study was to assess the influence of key parameters on CFPT 's behavior under compression load. This was fulfilled by establishing a database of 175 test points from twenty-one paper [2,6,7, 12-29] and was supplemented by the 9 test results of the present study, Table 1. Statistical indexes were used to evaluate the influence of major key parameters on the performance of CFPT columns under compression load.

2. Experimental investigation

Ordinary Portland cement similar to Type I Portland cement (ASTM) (150-89) with a specific gravity of 3.15 was used. The fine aggregate was river sand from the Eski-kalak region with a specific gravity of 2.6. The coarse aggregate was from the same source with a maximum specific gravity of 2.65. Using carpentry machines, uPVC tube with an overall diameter of 150mm was cut to the required heights (300mm), and the ends were grinded. The tubes were assembled in a horizontal timber mold supported by a sizeable vibrating table. A rotary drum concrete mixer was used for mixing the concrete ingredients with a mix ratio of 1:2:4, w/c of 0.62, and a maximum aggregate size of 14mm to achieve a target compressive strength of 25 N/mm^2. The specimens were filled with fresh concrete from the drum mixer in three layers, and each layer was compacted for 30 seconds. The finished surfaces were troweled and covered with plastic sheets for 24 hours. A similar number of control specimens (9) were cast in steel molds. After 24hours, the control specimens were de-molded and grouped into three sets of three specimens. Each set was cured in the laboratory for 28 days in the open air (CFPT-A) or water (CFPT-W) or sealed in a chamber (CFPT-S), Fig.1. At the end of the curing period, the specimens were tested under monotonic axial compression load, and the test results were tabulated in Table 1.

Table 1. Database of experimental results for CFPT from literature and present study.

Reference	Specimen	ρs	fuc	ρsfy/fco	fccexp	α_{1Exp}=fcc /fuc	p_b=2fup t/D	α2=fcc-fuc/p_b	α3=Apfy p/Acfuc
Kurt (1978) [12]	3c	0.31	21.37	0.507	40.1	1.876	5.166	3.62	0.508
	6c	0.315	20.6	0.535	40.1	1.94	5.24	3.7	0.535
	7c	0.315	20.6	0.535	39.2	1.9	5.24	3.5	0.535
Maiturare (1990) [13]	A41	0.129	26.24	0.172	30.58	1.37	2.66	1.63	0.172
	A42	0.129	26.24	0.172	30.58	1.37	2.66	1.63	0.172
	A43	0.129	26.24	0.172	30.58	1.37	2.66	1.63	0.172
	A31	0.129	22.32	0.202	29.1	1.3	2.66	2.55	0.203
	A32	0.129	22.32	0.202	29.5	1.32	2.66	2.7	0.203
	A33	0.129	22.32	0.202	28.7	1.28	2.66	2.4	0.203
	A71	0.102	18.4	0.19	27.84	1.51	2.36	4	0.194
	A72	0.102	18.4	0.19	28.5	1.55	2.36	4.28	0.194
	A73	0.102	18.4	0.19	27.84	1.51	2.36	4	0.194
	B31	0.129	20.84	0.216	31.8	1.52	2.66	4.12	0.217
	B32	0.129	20.84	0.216	31.9	1.53	2.66	4.16	0.217
	B33	0.129	20.84	0.216	32	1.54	2.66	4.2	0.217
	B41	0.129	22.21	0.203	33	1.486	2.66	4.05	0.204
	B42	0.129	22.21	0.203	33	1.486	2.66	4.05	0.204
	B43	0.102	22.21	0.16	33	1.486	2.36	4.05	0.204
	B71	0.102	21.04	0.16	30.7	1.45	2.36	4.09	0.17
	B72	0.102	21	0.17	30.7	1.46	2.36	4.11	0.17
	B73	0.129	21	0.215	30.7	1.46	2.66	4.11	0.17
Marzouck and Sennah (2002) [14]	3	0.129	33.7	0.134	39.2	1.17	2.66	2.07	0.134
	5	0.129	36.5	0.123	40.515	1.11	2.66	1.51	0.124
Saadoon (2010) [15]	220A1-24.1	0.127	19.5	0.228	27.6	1.42	2.88	2.8	0.228
	220B1-23.7	0.207	18.8	0.385	31.7	1.688	4.78	2.7	0.418
	220A2-3.4	0.127	32.8	0.135	36.6	1.12	2.88	1.32	0.136
	220B2-39.0	0.207	31.6	0.229	41.9	1.326	4.78	2.15	0.249
	400A1	0.127	24	0.185	34.152	1.423	2.88	3.525	0.186
	600A1	0.127	24	0.185	34.32	1.43	2.88	3.55	0.186
	800A1	0.127	24	0.185	34.92	1.455	2.88	3.79	0.186
	400B1	0.207	23.7	0.305	40.48	1.708	4.78	3.51	0.331
	600B1	0.207	23.7	0.305	41.14	1.736	4.78	3.65	0.331
	800B1	0.207	23.7	0.305	42.87	1.809	4.78	4.01	0.331
	400A2	0.127	39.4	0.113	44.13	1.12	2.88	1.64	0.113
	600A2	0.127	39.4	0.113	44.325	1.125	2.88	1.71	0.113
	800A2	0.127	39.4	0.113	45.31	1.15	2.88	2.05	0.113
	400B2	0.207	39	0.186	51.87	1.33	4.78	2.69	0.201
	600B2	0.207	39	0.186	52.689	1.351	4.78	2.86	0.201
	800B2	0.207	39	0.186	53.35	1.368	4.78	3	0.201
Jiang et al. (2012)[16]	ZD-0	0.096	29.76	0.113	31.18	1.048	1.98	0.717	0.113
Wang and Yang (2012) [2]	PVC0.6–C30	0.145	18.2	0.358	30.59	1.681	3.03	4.089	0.358
	PVC1.0–C30	0.145	18.2	0.358	34.9	1.981	3.03	5.5	0.358
	PVC1.6–C30	0.145	18.2	0.358	42.68	2.345	3.03	8.08	0.358
	PVC0.6–C45	0.22	27.32	0.362	36.17	1.324	4.25	2.08	0.362
	PVC1.0–C45	0.22	27.32	0.362	41.26	1.551	4.25	3.28	0.362
	PVC1.6–C45	0.22	27.32	0.362	45.55	1.668	4.25	4.289	0.362
	PVC0.6–C60	0.399	49	0.366	49.54	1.011	6.95	0.077	0.366
	PVC1.0–C60	0.399	49	0.366	49.7	1.014	6.95	0.1	0.366
	PVC1.6–C60	0.399	49	0.366	49.95	1.019	6.95	0.137	0.366
Gupta (2013) [17]	T160M20PC-1	0.115	23.6	0.25	31.62	1.34	2.76	2.9	0.206
	T160M20PC-2	0.115	23.6	0.205	31.86	1.35	2.76	3	0.206
	T200M20PC-1	0.128	23.6	0.216	32.56	1.38	3.04	2.95	0.229
	T200M20PC-2	0.128	23.6	0.216	33.28	1.41	3.04	3.18	0.229
	T140M25PC-1	0.121	28.6	0.178	34.32	1.2	2.89	1.98	0.179
	T140M25PC-2	0.121	28.6	0.178	33.18	1.16	2.89	1.58	0.179
	T140M40PC-1	0.121	43.5	0.117	46.5	1.07	2.89	1.04	0.118
	T140M40PC-2	0.121	43.5	0.117	48.29	1.11	2.89	1.66	0.118
Soliman (2013) [18]	SCC6-30	0.138	13.75	0.351	32.59	2.37	3.32	5.67	0.351
	SCC6-40	0.138	12.1	0.399	27.1	2.24	3.32	4.52	0.399
	SCC6-60	0.138	11.6	0.416	25.75	2.22	3.32	4.26	0.417
	SCC6-90	0.138	9.1	0.53	21.75	2.39	3.32	3.81	0.531
	SCC5-20	0.149	13.75	0.379	35.75	2.6	3.56	6.18	0.352

(*Table 1 Cont.)*

	SCC5-30	**0.149**	**11.9**	**0.438**	**29.63**	**2.49**	**3.56**	**4.98**	**0.406**
	SCC5-60	0.149	9.5	0.548	26.6	2.8	3.56	4.8	0.55
	SCC5-90	0.149	9	0.57	26.1	2.9	3.56	4.8	0.581
Abdulla (2014) [19]	1	0.202	60.26	0.167	74.72	1.24	6.03	2.4	0.21
	2	0.202	47.92	0.21	67.57	1.41	6.03	3.26	0.264
	3	0.202	39.28	0.257	47.14	1.2	6.03	1.3	0.322
	4	0.202	34.92	0.289	42.25	1.21	6.03	1.21	0.362
	5	0.202	33.07	0.305	40.68	1.23	6.03	1.26	0.382
	6	0.202	31.15	0.324	35.8	1.15	6.03	0.77	0.406
	7	0.202	30.9	0.326	36.46	1.18	6.03	0.92	0.409
	8	0.202	29.85	0.338	34.92	1.17	6.03	0.84	0.424
	9	0.202	27.47	0.367	34.34	1.25	6.03	1.14	0.46
	10	0.202	27.81	0.363	33.1	1.19	6.03	0.877	0.454
	11	0.202	26.2	0.385	31.96	1.22	6.03	0.955	0.483
	1	0.234	59.35	0.197	73	1.23	5.65	2.416	0.198
	2	0.234	47.62	0.245	65.72	1.38	5.65	3.2	0.246
	3	0.234	39.1	0.299	45.75	1.17	5.65	1.177	0.3
	4	0.234	32.89	0.355	42.1	1.28	5.65	1.63	0.356
	5	0.234	31.55	0.37	39.44	1.25	5.65	1.396	0.372
	6	0.234	31.2	0.375	38.69	1.24	5.65	1.32	0.376
	7	0.234	30.21	0.387	36.86	1.22	5.65	1.177	0.388
	8	0.234	28.97	0.403	35.63	1.23	5.65	1.178	0.405
	9	0.234	27.35	0.427	34.74	1.27	5.65	1.3	0.429
	10	0.234	25.77	0.454	33.5	1.3	5.65	1.368	0.455
	11	0.234	24.49	0.477	30.86	1.26	5.65	1.127	0.479
	1	0.21	56.41	0.186	70.5	1.25	5.14	2.74	0.186
	2	0.21	48.04	0.218	60.05	1.25	5.14	2.34	0.218
	3	0.21	34.16	0.307	42.7	1.25	5.14	1.66	0.307
	4	0.21	32.26	0.325	41.29	1.28	5.14	1.75	0.325
	5	0.21	31.12	0.337	37.65	1.21	5.14	1.27	0.34
	6	0.21	33.02	0.318	37.3	1.13	5.14	0.83	0.318
	7	0.21	30.13	0.348	35.55	1.18	5.14	1.05	0.348
	8	0.21	29.64	0.354	35.57	1.2	5.14	1.15	0.354
	9	0.21	28.17	0.372	32.68	1.16	5.14	0.877	0.373
	10	0.21	25.94	0.404	31.64	1.22	5.14	1.11	0.404
	11	0.21	24.11	0.435	30.14	1.25	5.14	1.17	0.435
Fakharifar et al. (2014) [6]	CFT-40W	0.217	52	0.172	52.6	1.05	4.7	0.127	0.172
	CFT-40G	0.217	52	0.172	49.5	1	4.7	0.53	0.172
	CFT-80G	0.217	52	0.172	47.8	0.97	4.7	0.89	0.172
Oyawa et al. (2015) [20]	C/C20/110/2	0.098	8.9	0.385	17.5	1.97	1.82	4.72	0.383
	C/C20/110/3	0.098	7.4	0.463	17.17	2.32	1.82	5.368	0.461
	C/C20/83/2	0.162	8	0.708	24.32	3.04	2.89	5.64	0.708
	C/C20/83/3	0.162	6.9	0.82	22.56	3.27	2.89	5.42	0.821
	C/C20/83/4	0.162	6.1	0.929	22.27	3.65	2.89	5.59	0.929
	C/C20/55/2	0.21	9.9	0.742	25.25	2.55	3.63	4.22	0.742
	C/C20/55/3	0.21	9.1	0.807	24.66	2.71	3.63	4.28	0.808
	C/C20/55/4	0.21	7.8	0.942	23.1	2.96	3.63	4.21	0.942
	C/C25/110/2	0.21	16	0.459	19.2	1.2	1.82	1.758	0.459
	C/C25/110/3	0.21	14.5	0.57	18.13	1.25	1.82	1.99	0.507
	C/C25/83/2	0.162	14.3	0.396	26.03	1.82	2.89	4.05	0.396
	C/C25/83/3	0.162	12	0.47	24.6	2.05	2.89	4.36	0.472
	C/C25/83/4	0.162	10.7	0.53	23.97	2.24	2.89	4.59	0.529
	C/C25/55/2	0.21	20	0.367	28.4	1.42	3.64	2.3	0.367
	C/C25/55/3	0.21	15.7	0.468	27	1.72	3.64	3.1	0.468
	C/C25/55/4	0.21	12.2	0.602	23.3	1.91	3.64	3.05	0.602
	C/C30/110/2	0.21	17.4	0.422	20.53	1.18	1.82	1.72	0.422
	C/C30/110/3	0.21	14.6	0.503	18.98	1.3	1.82	2.4	0.503
	C/C30/83/2	0.162	14.7	0.385	26.75	1.82	2.89	4.17	0.385
	C/C30/83/3	0.162	13.5	0.42	25.11	1.86	2.89	4.02	0.42
	C/C30/83/4	0.162	12.8	0.443	24.6	1.92	2.89	4.08	0.442
	C/C30/55/2	0.21	20.9	0.351	29.26	1.4	3.64	2.296	0.351
	C/C30/55/3	0.21	18.4	0.399	27.78	1.51	3.64	2.57	0.40
	C/C30/55/4	0.21	14.4	0.51	26.35	1.83	3.64	3.28	0.51

(*Table 1 Cont.)*

Osman and Soliman (2015) [21]	**PVC-20**	**0.149**	**13.75**	**0.433**	**35.5**	**2.58**	**3.65**	**5.96**	**0.434**
	PVC-30	0.149	11.9	0.5	33.32	2.8	3.65	5.87	0.502
	PVC-60	0.149	9.5	0.627	22.8	2.4	3.65	3.64	0.629
	PVC-90	0.149	9	0.662	25.2	2.8	3.65	4.43	0.66
Fakharifar and Chen (2016) [7]	CFPT-G40#1	0.193	49.5	0.161	52.47	1.06	4.3	0.69	0.161
	CFPT-G40#2	0.193	49.5	0.161	49.5	1	4.3	0	0.161
	CFPT-G40#3	0.193	49.5	0.161	48.02	0.97	4.3	-0.344	0.161
Abhale et al. (2016) [22]		0.145	11.51	0.44	15.77	1.37	2.62	1.626	0.44
		0.145	12.1	0.419	16.2	1.34	2.62	1.56	0.42
		0.145	11.6	0.437	15.78	1.36	2.62	1.595	0.438
		0.145	11	0.461	14.96	1.36	2.62	1.51	0.462
Kumutha and Vijai 2016 [23]		0.084	18.06	0.162	21.3	1.18	2.03	1.59	0.162
		0.102	18.06	0.197	25.83	1.43	2.7	2.87	0.162
		0.066	18.48	0.125	22.73	1.23	1.73	2.46	0.134
		0.096	18.48	0.182	26.6	1.44	2.31	3.51	0.182
Mammen and Antony (2017) [24]	II	0.099	26	0.133	28	1.077	1.85	1.08	0.133
	III	0.15	26	0.202	29	1.115	2.7	1.11	0.202
	IV	0.259	26	0.348	30	1.154	4.35	0.92	0.348
Karthikeyan et al. (2018) [25]	PVC	0.138	28.98	0.166	37	1.277	2.5	3.2	0.167
		0.138	28.36	0.17	35.15	1.239	2.5	2.716	0.17
		0.138	29.6	0.163	35.77	1.21	2.5	2.468	0.163
	UPVC	0.3	28.98	0.362	47.73	1.65	4.9	3.82	0.361
		0.3	28.36	0.37	51.55	1.82	4.9	4.73	0.37
		0.3	29.6	0.354	44.46	1.5	4.9	3.03	0.354
Azzez et al. (2018) [26]	PC20t1	7857	21.2	0.15	27.36	1.29	3.458	1.78	0.239
	PC20t2	7857	21.2	0.2	29.01	1.37	4.74	1.65	0.332
	PC25t1	7857	24.16	0.15	29.88	1.24	3.458	1.654	0.21
	PC25t1	7857	24.16	0.2	31.46	1.3	4.74	1.54	0.29
	PC40t1	7857	40.12	0.15	41.85	1.4	3.458	0.5	0.126
	PC40t1	7857	40.12	0.2	43.6	1.09	4.74	0.73	0.175
Woldermariyaem et al. (2019) [27]	C1P1H1	3119	10.35	0.17	24.38	2.356	3.948	3.554	0.649
	C1P2H1	6364	10.35	0.14	23.08	2.231	3.316	3.839	0.542
	C1P3H1	9507	10.35	0.11	22	2.127	2.713	4.294	0.441
	C1P4H1	15400	10.35	0.09	20.99	2.029	2.132	4.99	0.344
	C2P1H1	3119	13.79	0.17	27.47	1.992	3.948	3.465	0.487
	C2P2H1	6364	13.79	0.14	26.8	1.943	3.316	3.923	0.407
	C2P3H1	9507	13.79	0.11	24.93	1.808	2.713	4.106	0.331
	C2P4H1	15400	13.79	0.09	23.76	1.722	2.132	4.676	0.258
	C3P1H1	3119	16.89	0.17	28.72	1.7	3.948	2.996	0.398
	C3P2H1	6364	16.89	0.14	28.48	1.686	3.316	3.495	0.332
	C3P3H1	9507	16.89	0.11	26.99	1.598	2.713	3.723	0.27
	C3P4H1	15400	16.89	0.09	24.57	1.454	2.132	3.602	0.211
	C4P1H1	3119	20.13	0.17	32.13	1.596	3.948	3.04	0.333
	C4P2H1	6364	20.13	0.14	30.68	1.524	3.316	3.182	0.278
	C4P3H1	9507	20.13	0.11	29.66	1.473	2.713	3.513	0.227
	C4P4H1	15400	20.13	0.09	28.01	1.391	2.132	3.696	0.177
	C5P1H1	3119	24.12	0.17	34.73	1.44	3.948	2.687	0.278
	C5P2H1	6364	24.12	0.14	34.31	1.423	3.316	3.073	0.232
	C5P3H1	9507	24.12	0.11	32.77	1.358	2.713	3.188	0.189
	C5P4H1	15400	24.12	0.09	30.87	1.28	2.132	3.166	0.148
Abdulla [28]	ST-PT1-1	0.38	44.1	0.39	53.2	1.2	4.75	1.91	0.21
Abdulla [29]	S1	0.42	30.5	0.6	42.62	1.39	3.77	3.20	0.23
Present study	CFPT-A1	0.154	24.3	0.27	32.8	1.39	3.36	2.53	0.27
	CFPT-A2	0.154	24.3	0.25	33.7	1.33	3.36	2.5	0.25
	CFPT-A3	0.154	24.3	0.263	35.1	1.45	3.36	3.27	0.263
	CFPT-W1	0.154	25.4	0.248	33.5	1.31	3.36	2.38	0.248
	CFPT-W2	0.154	25.4	0.26	33.9	1.39	3.36	2.86	0.26
	CFPT-W3	0.154	25.4	0.239	34.6	1.31	3.36	2.47	0.239
	CFPT-S1	0.154	26.0	0.243	33.3	1.28	3.36	2.17	0.243
	CFPT-S2	0.154	26.0	0.251	34.1	1.35	3.36	2.65	0.251
	CFPT-S3	0.154	26.0	0.237	35.8	1.33	3.36	2.65	0.237

Fig. 1 CFPT specimens cured in (a) open air; (b) water; (c) sealed.

Vertical displacement was monitored using two linear displacement transducers, Fig.2. The experimental tests were conducted at a speed of 0.3mm/s, and the test was continued until the end of plastic stage was reached where the specimens underwent major plastic deformations.

Fig. 2 Testing of CFPT columns.

3. Results and discussions

3.1 Strength of tested CFPT

The confined strength of the three groups of CFPT is shown in Fig.3. Although there is a better performance for chamber sealed specimens, there is no clear trend on the influence of curing environment on CFPT due to the presence of plastic tube which acts as a continuous shell and reduces the environmental effects on the concrete core. This is ascribed to the fact that any moisture loss is overcome by the PVC tube, which influences the setting and hydration of fresh concrete. Furthermore, the concrete surface pores are closed by the tube and this positively influences the curing process. This capability of tube can confer an additional protective cover to concrete in aggressive environments (bridge columns and piers); and in moist surroundings (car parks).

3.2. Water absorption

The concrete cover is more vulnerable to moisture loss than the concrete core. Thus, the water absorption of surface concrete is usually higher than core concrete due to the rapid loss of water in the cover concrete during curing. Water absorption is used to determine the role of plastic tube in hindering the amount of water absorbed by the concrete in water or moist environments. Absorption tests were carried out in accordance to ASTM C1585 – 20 at room temperature because the plastic tube is highly sensitive to heating in oven. The test results of water absorptions for CFPT and plain concrete specimens were plotted in Fig.4. Lower absorption value is observed for CFPT columns. The polymeric tube was effective in reducing the absorption capacity of specimens by more than 80%. Several factors affect the water absorption of CFPT specimens including type and thickness of plastic tube, strength of concrete core and exposure time. Fig.4 sheds light on the performance of the confining device in sealing concrete specimens in water or humid environments due to the uniformity in the surface of the plastic tube.

3.3. Tube confinement effect

Pressure from the applied load or internal pressure from in-filled-concrete causes the tube wall to be stressed. Permanent deformations resulted when stress in the tube wall allowed to reach the tube material's yield strength or tensile strength. Bursting pressure of tube may be determined approximately with Barlow's formula [30]:

$$p_b = \frac{2 f_{uP} t}{D} \quad (1)$$

where p_b=burst pressure, t= thickness of tube wall, D= outside diameter, and f_{uP}= tensile strength of tube material. Failure of the plastic tube happens when the confined pressure attains its burst pressure. The polymeric tube is a kind of high-strength plastic material [31]. The uPVC tube acts on the brittle circumferential concrete surface as a continuously ductile shell and retains concrete core components in place after they have been damaged.

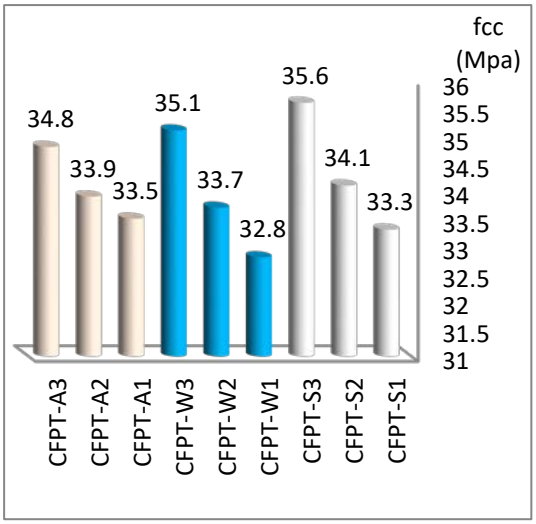

Fig.3 Strength of CFPT cured under the three different environmental conditions.

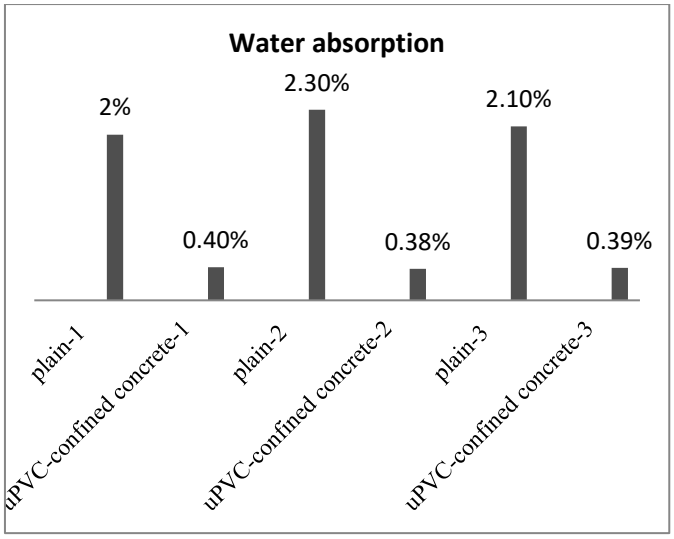

Fig. 4 water absorptions for tested PCC and plain concrete specimens.

4. Experimental database

An extensive review of the literature shows most of the previous studies have been performed on small specimens tested for a limited number of variables (one or two). Several features of CFPT remains not fully elucidated and requires more investigation. These include concrete strength, tube type, curing regimes, and length effect, with limited data on real-size specimens. The compiled database from nineteen studies and the test data of current study, Table 1, includes:

1) One hundred seventy-five test data from the published literature.
2) Test results for normal-strength (fuc≤40MPa) as well as the high-strength concrete (fuc>40MPa)
3) small-sized and larger specimens for the size effect
4) Plastic tube yielding was the failure mode for the specimens included in the database.
5) Data extremely deviate from the overall trend of the whole data was ignored.
6) No specimens with steel reinforcement
7) Parameters that related to the tube geometry; thickness (t), depth (d), height (h), h/d, h/t, d/t ratios) and mechanical properties yield strength (fyp), ultimate tube strength (fup), and modulus of elasticity of tube (Ep).
8) Some relevant details when was not given it was assumed as follows: f_{yp}=35MPa, f_{up}=45MPa, E_p=3000MPa.

4.1 Database parameters

An attempt was made to assemble a more extensive test database from the published literature combined with the present test results. The performance of each parameter in the database was then evaluated using the statistical indexes. The critical parameters considered by the current study and other details of the test database are shown in Table 1.

4.2 Strength index (α1)

Three indexes were used to evaluate the change in concrete due to plastic tube presence relative to confinement effect (α_1), burst pressure (α_2), and geometric and mechanical properties of the materials (α_3). The strength index α_1 was computed from:

$$\alpha_1 = \frac{f_{cc}}{f_{uc}} \tag{2}$$

All α_1 values, the strength enhancement ratio, summarized in Table 1. Specimens with full jacketing were considered. Specimens with gap at top and bottom were excluded. Using the PVC jacket, the maximum increase in concrete strength confinement was about 365% [20]. Both laboratory testing and site investigations have shown

the tube to be a simple yet effective means to enhance the deformation and bearing capacity of concrete and improve its durability [1].

4.3 α_1 –fuc relationship

The distribution of unconfined concrete compressive strengths for the assembled database is shown in Fig.5, where the failure is controlled by the compression crushing of concrete. The unconfined concrete strength (fuc), as obtained from concrete cylinder tests, varied from 6.1 to 62MPa. A majority of the data results were in the range of 20–40 MPa. The compressive strength of concrete exhibited an inverse relationship with α_1. An increase in unconfined concrete strength *f*uc was accompanied by a decrease in strength enhancement ratio *fcc/fuc*. A reasonable correlation was obtained between α_1 and f_{uc} yielding the following equation:

$$\alpha_1 = 6.28(f_{uc})^{-0.46} \qquad R^2=0.69 \tag{3}$$

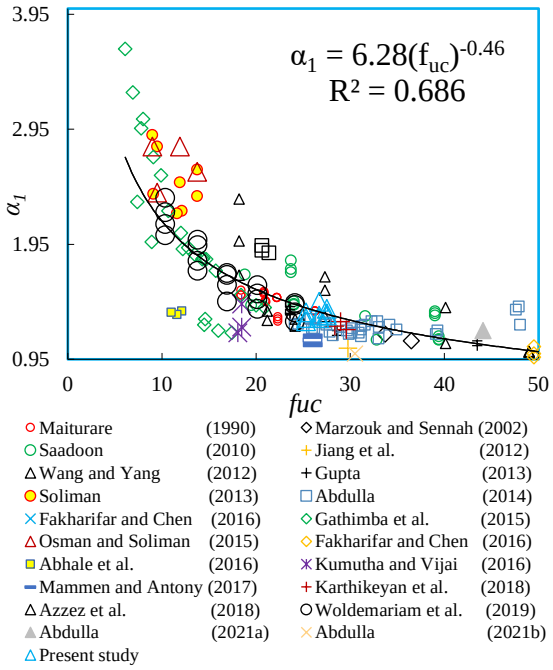

Fig.5 Strength index α_1, the effect of fuc.

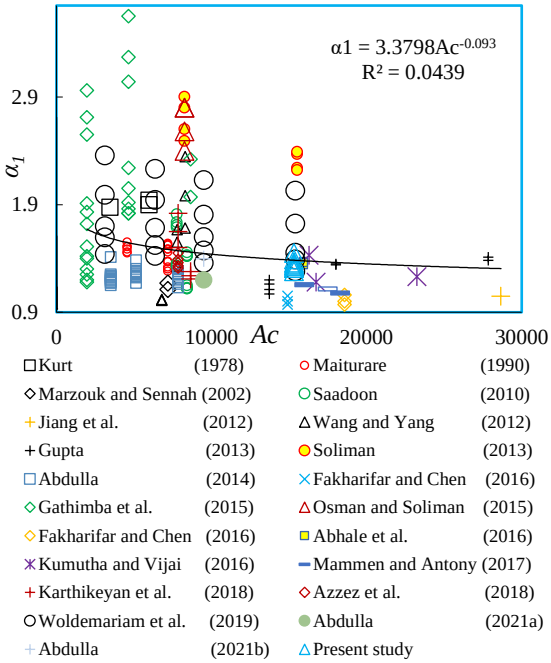

Fig.6 Strength index α_1, the effect of Ac.

4.4 $\alpha_1$variations with Ac

Despite the scatter of results, α_1 decreases with increase in area of concrete (Ac) up to a value of 15000mm^2, Fig. 6. Beyond this value, the increase in A_C would have a marginal effect on strength enhancement.

4.5 α_1–dp relationship

The influence of tube diameter (dp) on the axial behavior of CFPT is shown in Fig. 7. The large scatter in test data might be explained by the specimen's geometrical imperfections. Most of the specimens in the database were in the range of 75-150mm. Fig.7 shows that increasing the column diameter decreased the confinement contribution on the axial capacity of CFPT.

4.6 α_1–t relationship

The influence of tube thickness (t_p) on the strength enhancement followed a similar trend to that of *dp*, Fig.8. This shows that up to a certain thickness, 4mm, the tube effectively improves the strength of CFPT. Beyond this thickness, the benefit of enhancement in strength diminishes with the increase in tube thickness.

4.7 α_1–Ap relationship

The effect of change in tube cross-sectional area (Ap) on α_1 depicted in Fig.9. A wide range of Ap is covered in the database, where the parameter under consideration exhibits a reverse relationship with the index α_1. Despite this clear trend, the correlation between the two is weak.

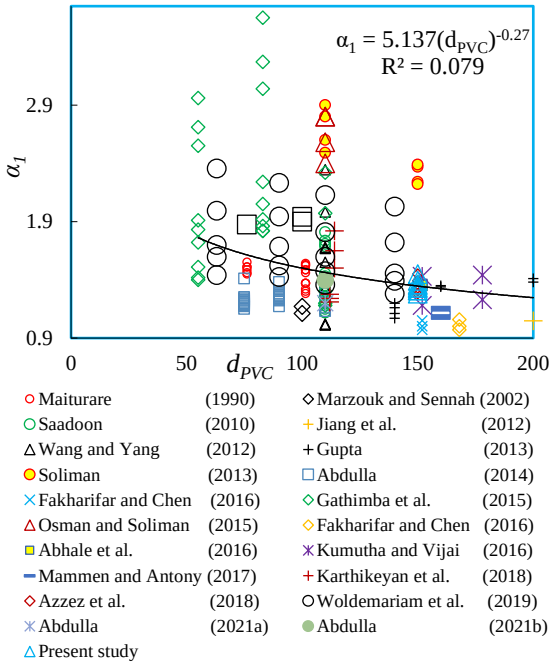

Fig.7 Strength index $\alpha_1$variation with d_P.

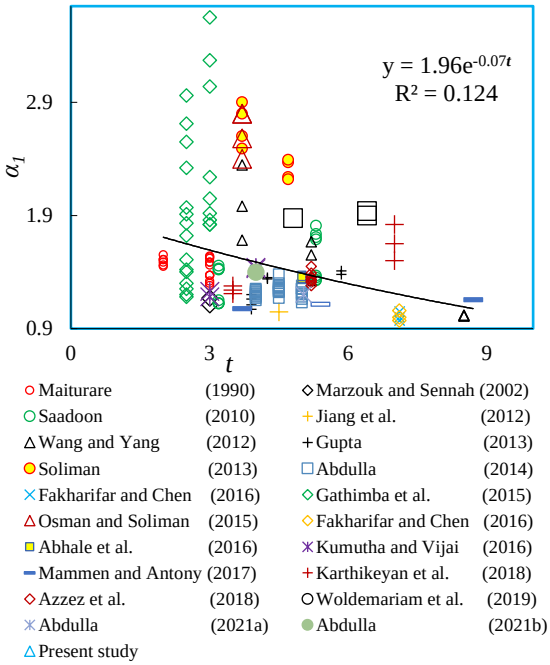

Fig.8 Strength index α_1 variation with t_p.

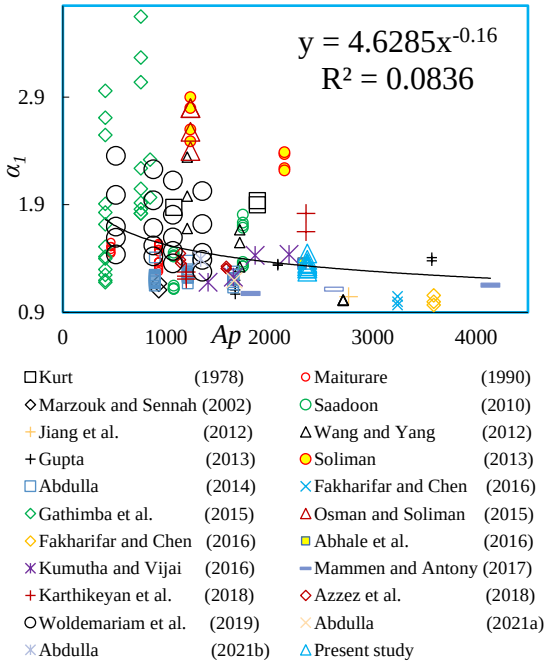

Fig.9 Strength index α_1, the effect of Ap.

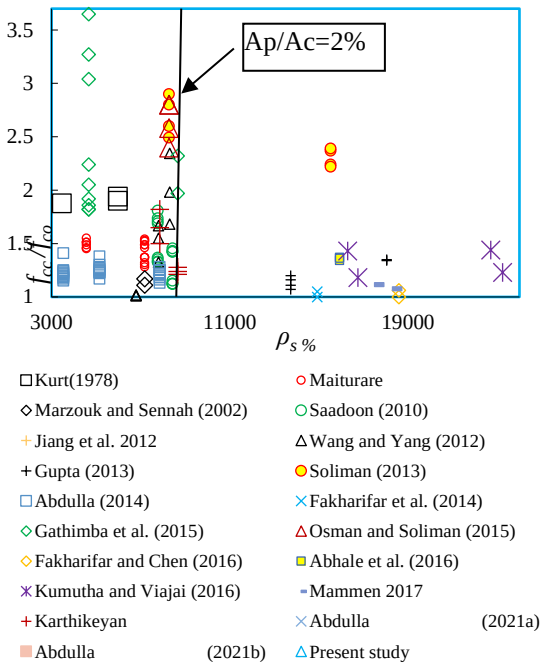

Fig.10 Strength index α_1, the effect of ρ_p.

4.8 $\alpha_1$variations with ρ_p

Fig. 10 depicts the relationship between the index α_1 and plastic reinforcement ratio (ρ_p) expressed by *Ap/Ac* ratio. For confinement efficiency, the effective rate of ρ_p lies in the range of 1 to 2%. Beyond this ratio, strength enhancement becomes uneconomical.

4.9 α_1–f_{yp} relationship

Fig. 11 shows the influence of tube mechanical properties on the strength enhancement parameter. The effect on α_1 with change in f_{yp} is depicted in Fig.11, where α_1 reduces with higher yield values of the plastic tube. The data in Fig. 11 is grouped into several small zones. Most of the specimens yielded in the range 35-45MPa.

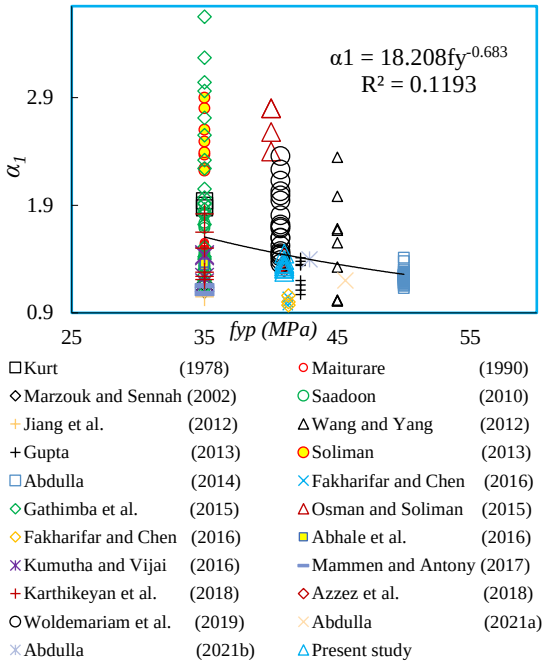

Fig.11 Strength index α_1, influence of *fyp*.

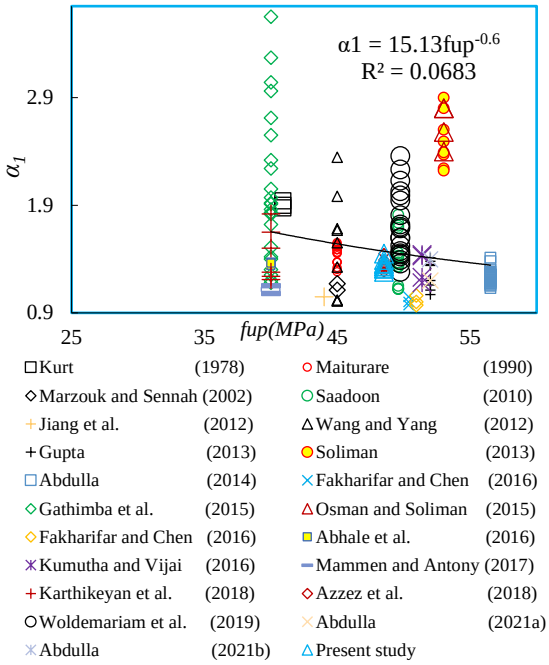

Fig.12 Strength index α_1, the influence of *fup*.

4.10 α_1 variations with f_{up}

The effect of ultimate tensile strength (f_{up}) of plastic tube on α_1 is shown in Fig. 12. Despite the weak correlation, the strength enhancement decreased with an increase in *fup*.

4.11 α_1–E_p relationship

Fig. 13 depicts the relationship between the modulus of elasticity of tube (E_p) and the index α_1. Despite the low correlation between these parameters, the strength enhancement reduces with the increase in tube stiffness. The low modulus uPVC acts as a protective jacket to the encased concrete core. Due to the random nature of E_p, it was hard to find an equation relating the stiffness to the strength index.

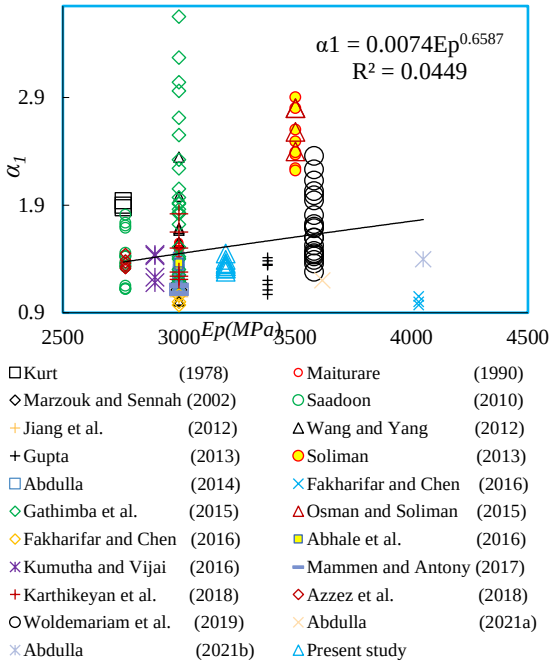

Fig.13 Strength index α_1, the influence of Ep.

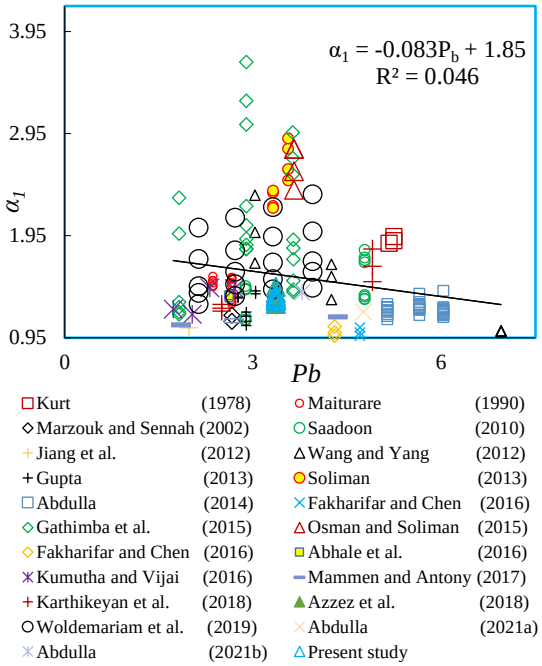

Fig.14 Strength index α_1, the influence of p_b.

4.12 α_1 variations with p_b

The effect of burst pressure (p_b) on the strength index is plotted in Fig.14. Although the assembled test data do not support a specific trend, it can be seen that increase in p_b has a negative influence on α_1.

4.13 Effect of geometric ratios

The effect of specimen geometry on strength index is shown in Fig.15. Specimens with an aspect ratio, height/diameter (h/d), of up to eight were covered in the database. However, most specimens' aspect ratio lay in the practical range of 2-4 (Fig. 15a). The height/diameter (h/t) ratio exhibited a similar trend to h/d, with a large scatter in test data, Fig.15b. The results for the diameter/thickness ratio (d/t) were less scattered and covered a wide range, 13 to 60, Fig.15c. The effect of the d/t ratio becomes marginal beyond a value of 45. Overall, a poor correlation was observed between the three geometric ratios and the strength index.

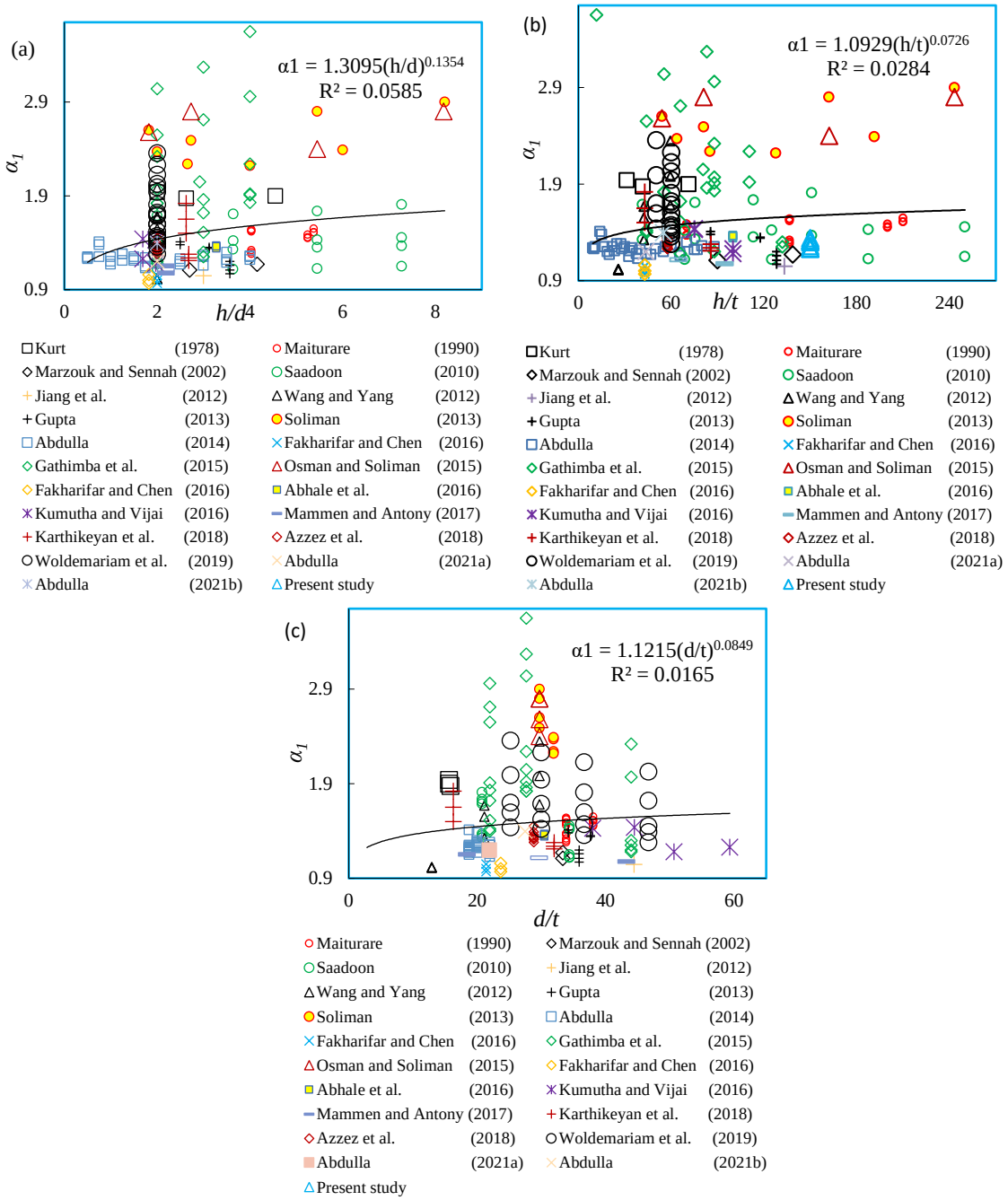

Fig. 15 Strength index α_1, influence of geometric ratios: (a) h/d; (b) h/t; (c) d/t.

4.14 Index α_1 and the influence of h and fcc

There was a very weak correlation between α_1 and h due to the scatter in test data, Fig. 16a. A better relationship was observed between α_1 and the confined strength (fcc), Fig. 16b, where α_1 reduced as fcc increased.

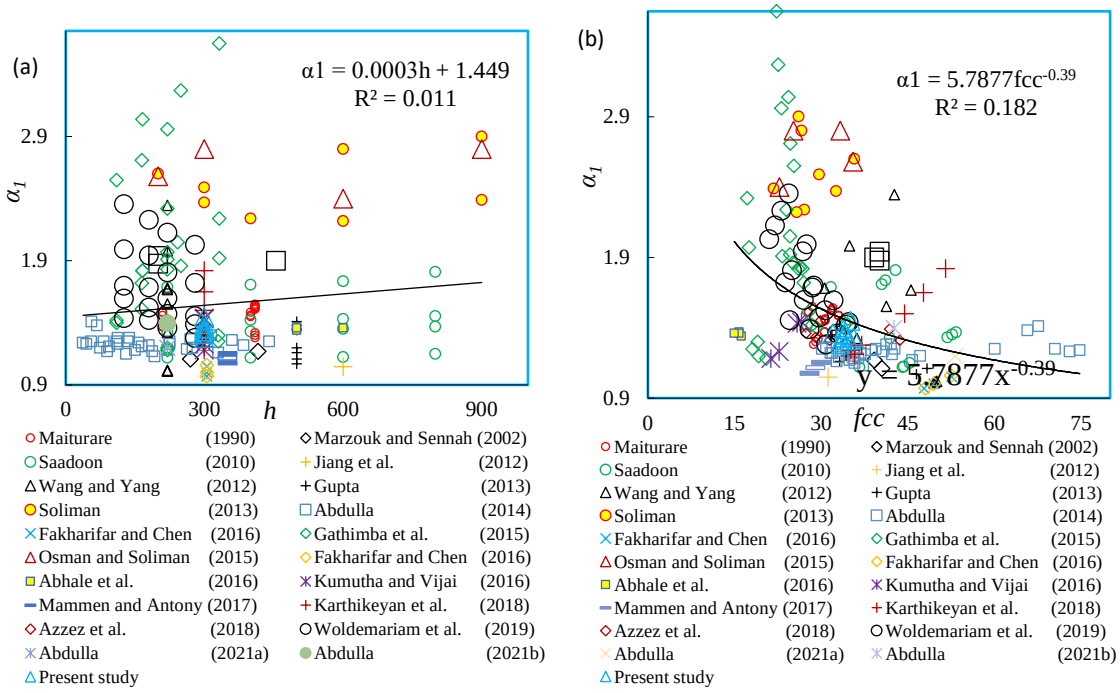

Fig. 16 Strength index α_1, effect of: (a) h; (b) fcc.

4.15 α_1 variation with α_2 and α_3

It was noticed that the first index was strongly related to α_2 and less affected by α_3 such that there was always a different optimum value for the first index relative to the other two indexes. The correlation coefficient between α1 and α3 was close to 0.53.

The second index (α_2) was given by:

$$\alpha_2 = \left[\frac{(\frac{P_u}{A} - f_{uc})}{p_b}\right] \tag{4}$$

where *Pu= fcc. A*= ultimate axial capacity of CFPT. where *A*=cross-sectional area of CFPT. Whereas the index (α_3) was given by:

$$\alpha_3 = \left(\frac{f_{yP} A_P}{f_{uc}\, A_c}\right) \tag{5}$$

where f_{yP} = yield strength of plastic tube; A_P =cross-sectional area of a plastic tube; *Ac* = area of the concrete core. The relationship between α_1 and α_2 was shown in Fig. 17(a), yielding a reasonable correlation expressed by:

$$\alpha_1 = 0.96e^{0.157(\alpha_2)} \qquad R^2=0.72 \tag{6}$$

In contrast to α_2, index α_3 displayed less influence on α_1 as shown graphically in Fig. 17(b) and expressed by the equation:

$$\alpha_1 = 2.5(\alpha_3)^2 + 0.15\alpha_3 + 1.16 \qquad R^2=0.57 \tag{7}$$

To eliminate the influence of geometric slenderness, specimens with a height-to-diameter (h/d) ratio greater than two were removed from the database. A better correlation between α_1 and α_2 was observed as shown in Fig. 18, yielding the following expression:

$$\alpha_1 = 0.993e^{0.14(\alpha_2)} \qquad R^2=0.79 \tag{8}$$

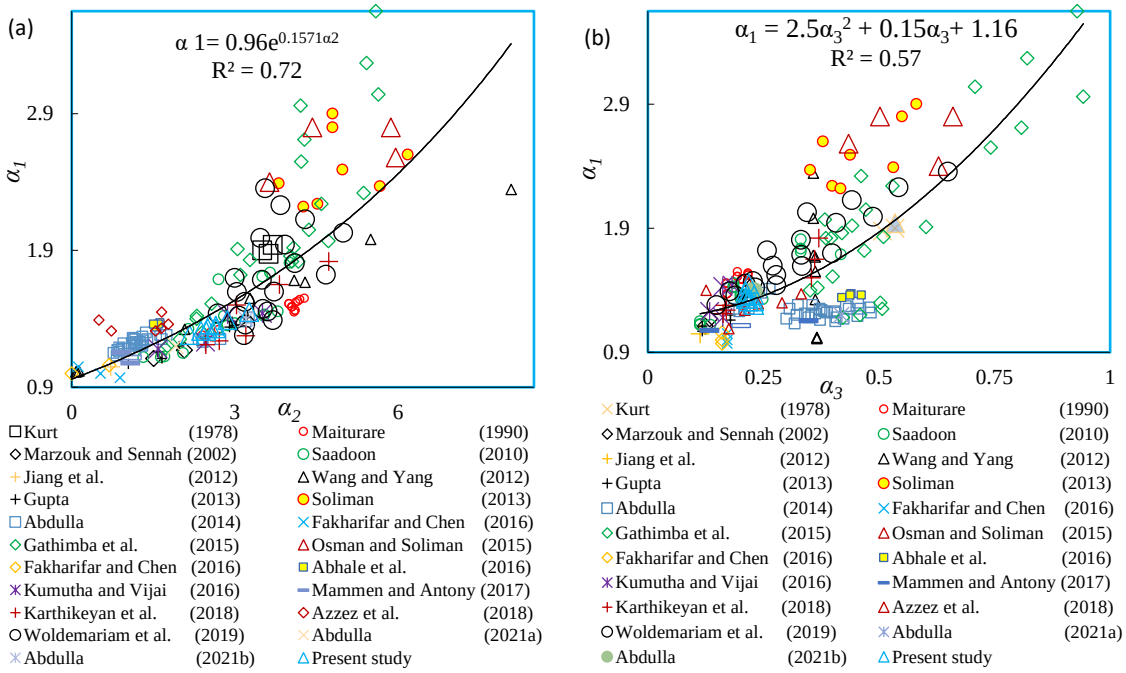

Fig. 17. Relationship between index α_1 and: (a) α_2; (b) α_3.

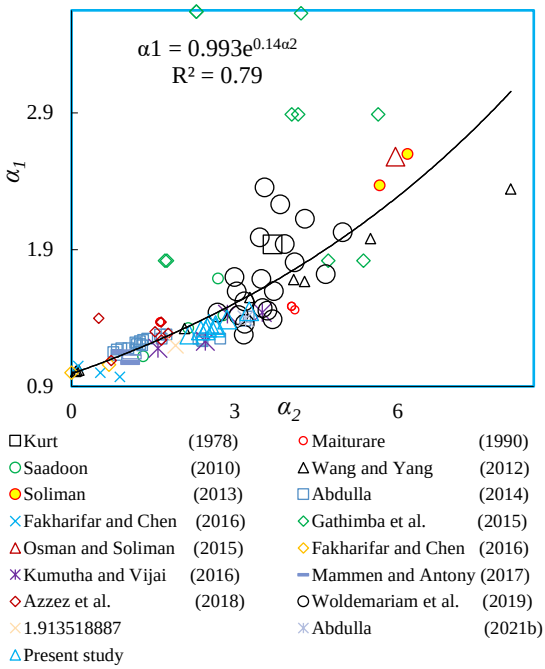

Fig.18 Variation of $\alpha_1$with α_2 for h/d=2.

4.16 Effect of p_b on α_2 and α_3

The variation of the two indexes α_2 and α_3 with burst pressure was shown in Fig. 19(a) and 19(b). Despite the scatter in the test data, the influence of burst pressure on the two indexes reduces when the former attains higher values.

4.17 α_2-α_3 relationship

No direct relationship between the two strength indexes α_2 were α_3 was noticed due to the divergence in test data. This showed that the index α_2 was not dependent on α_3, Fig.20.

4.18 fcc-fuc relationship

The fcc variation to fuc was plotted in Fig. 21 (a) for all h/d ratios and Fig. 21 (b) for h/d ratios equal to two. A reasonably good correlation was observed in the two cases yielding the following expressions:

$$f_{cc} = 0.82f_{uc}+13.85 \quad R^2 = 0.8 \tag{9}$$

For h/d=2

$$f_{cc} = 0.84f_{uc}+13.4 \quad R^2 = 0.83 \tag{10}$$

For all h/d ratios, *where fcc*=compressive strength of CFPT; f_{uc}=compressive strength of unconfined concrete.

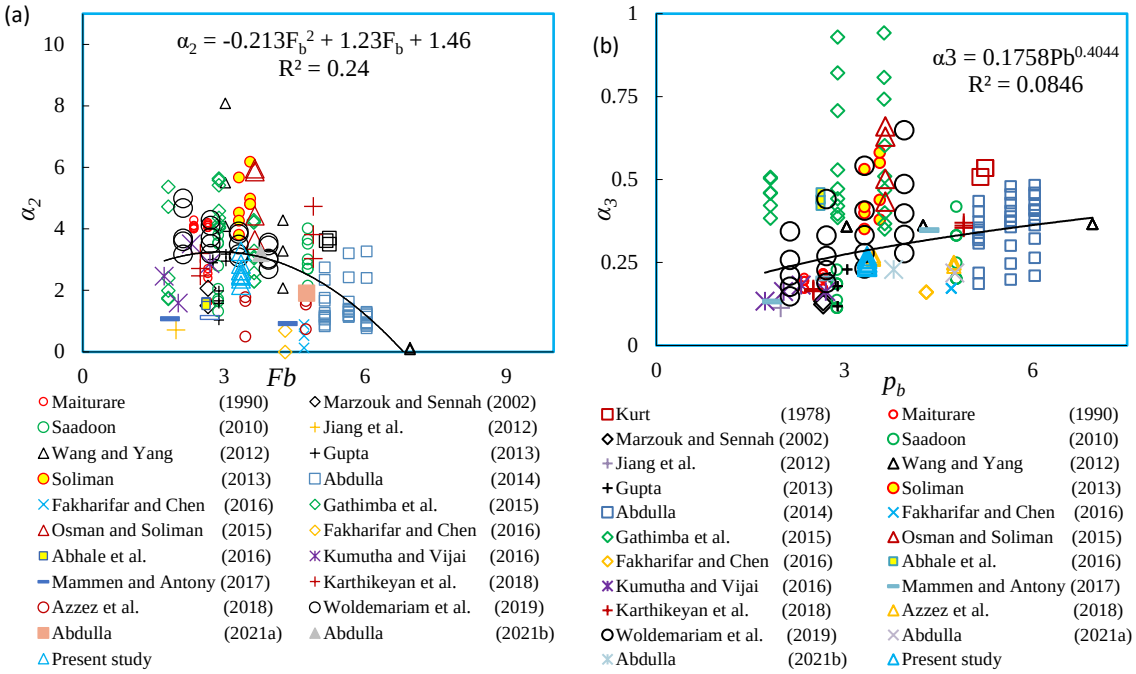

Fig. 19 Effect of p_b on: (a) α_2; (b) α_3.

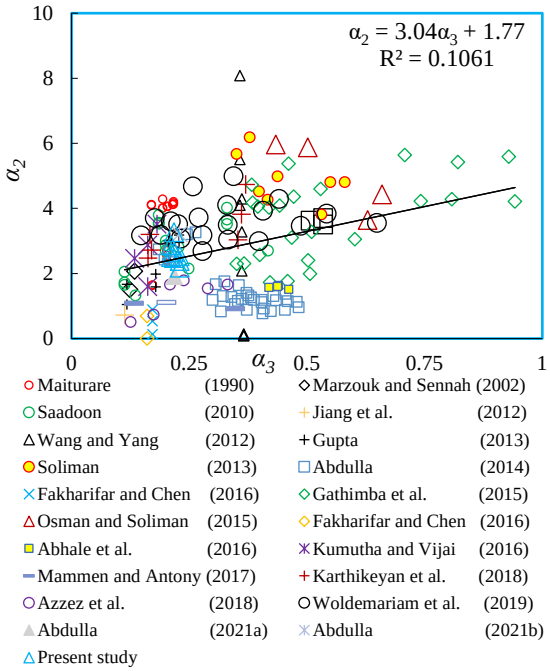

Fig. 20 α_2 versus α_3.

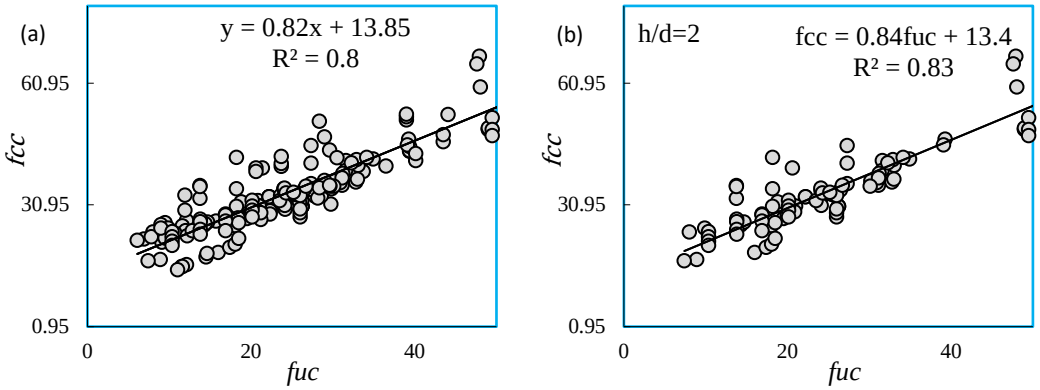

Fig. 21 fcc versus fuc for: (a) all h/d ratios in database; (b) h/d=2.

5. Conclusions

The strength capacity of short CFPT columns under different environmental conditions was investigated. The effect of three curing conditions, open-air, water, and sealed, on the CFPT specimens was examined. Furthermore, a test database on a broad framework was assembled for understanding the performance of CFPT under load. The database was supplemented by nine tests results of the present study. A detailed examination of different parameters affecting CFPT performance has yielded the following conclusions:

1) The performance of CFPT specimens under three different curing regimes was close, with the chamber sealed specimens performing better.

2) The plastic tube effectively reduced the water absorption of the confined concrete by more than 80%. The plastic tube acts as a continuous shell and reduces the environmental effects on the concrete core especially concrete shrinkage.

3) The uniaxial Compressive behavior of CFPT specimens in the database was considerably influenced by the compressive strength of in-fill concrete followed by the mechanical properties of the PVC tube.

4) The effect of the specimen's size was minimal. Compared with large specimens, small specimens exhibited slightly better behavior.

5) Specimens with higher strength showed lower ratios of strength index.

Most of the previous research covered a small number of samples. Future work should incorporate testing a larger number of specimens to ascertain the statistically significant trends more conclusively. Technical and engineering knowledge and sound construction expertise are necessary to promote plastic uPVC's safe and economic use.

6. References

[1] Abdulla NA. Concrete filled PVC tube: A review. Construction and Building Materials. 2017;156:321-329

[2] Wang JY, Yang QB. Investigation on compressive behaviors of thermoplastic pipe confined concrete. Construction and Building Materials. 2012;35: 578–585.

[3] Gupta PK, Verma VK. Study of concrete-filled un-plasticized polyvinyl chloride tubes in marine environment. Proc. Inst. Mech. Eng. Part M: J. Eng. Maritime Environ. 2016;230(2): 229-240.

[4] Abdulla NA. Influence of plastic pour-in form on mechanical behavior of concrete. 2019; 19: 193-202.

[5] J. Xue, H. Li, L. Zhai, X. Ke, W. Zheng, B. Men. Analysis on influence parameters and mechanical behaviors of embedded PVC pipe confined with reinforced high-strength concrete columns under cyclic reversed loading. Xi'an University of Arch. &Tech. (natural science edition). 2016;48(1).

[6] M. Fakharifar, G. Chen, Z. Lin, Z. T. Woolsey. Behavior and strength of passively confined concrete filled tubes. Tenth U.S. National Conference on Earthquake Engineering Frontiers of Earthquake Engineering. Alaska. 2014.

[7] Fakharifar M, Chen M.G. Compressive behavior of FRP-confined concrete filled PVC tubular columns. Compos. Struct. 2016;141:91–109.

[8] Feng Yu, Guoshi Xu, Ditao Niu, Anchun Cheng, Ping Wu, Zhengyi Kong. Experimental study on PVC-CFRP confined concrete columns under low cyclic loading. Construction and Building Materials. 2018;177:287–302.

[9] Abdulla NA. Energy Absorption Capacity of uPVC-Confined Concrete. Cement Based Composites. 2021; 2(2): 5559

[10] M. A. Raheemah, S. F. Resan. Structural behavior of slender PVC composite columns filled with concrete. IOP Conf. Ser. 2020.
[11] Vincent T, Ozbakkaloglu T. Influence of Shrinkage on Compressive Behavior of Concrete-filled FRP Tubes: An Experimental Study on Interface Gap Effect. Construction and Building Volume.2015;75: 144-156.
[12] Kurt E.C. Concrete filled structural plastic columns. Proceedings ASCE104 ST1. 1978.p.55–63.
[13] Maiturare F.D. Strength of Concrete Column Confined by Plastic Pipe (MS dissertation). Ahmadu Bello University, Zaria, 1990.
[14] Marzouck M., Sennah K. Concrete-filled PVC tubes as compression members, in: K.D. Ravindra, A.P. Kevin, D. Moray (Eds.), Proc. of International Congress: Challenges of Concrete Construction, New Cement Composite Materials for construction. Thomas Telford Limited, London, 2002. p. 31–38.
[15] Saadoon A.S. Experimental and Theoretical Investigation of PVC-Concrete Composite Columns (Doctoral dissertation). University of Basrah, Iraq. 2010.
[16] Jiang S, Dai T, Fu D, Wu Z, Li N. Experimental study on concrete columns confined by BFRP-PVC tubes under uniaxial loading. J Shenyang Jianzhu-Uni (Natural Science). 2012; 28(1): 23-29.
[17] Gupta PK. Confinement of concrete columns with un-plasticized Polyvinyl Chloride tubes. Int. J. Adv. Struct. Eng. 2013;5(19):1–8.
[18] Soliman AES. failure mechanism for confined plain concrete column. International Journal of Civil, Structural, Environmental and Infrastructure Engineering Research and Development.2013;3(5):249-268.
[19] Abdulla NA. Concrete filled Thermoplastic Tube under Compression. Proceedings of the 1st international Engineering conference on developments in civil and computer engineering applications, University of Ishik, Erbil, Iraq. 2014.p.60-70.
[20] Oyawa WO, Gathimba NK, Mang'uriu G.N. Innovative composite concrete filled plastic tubes in compression. The 2015 World Congress on Advances in structural engineering and mechanics (ASEM15). Incheon, Korea. 2015.
[21] Osman M, Soliman A. Behavior of Confined Columns under Different Techniques. International Journal of Civil, Environmental, Structural, Construction and Architectural Engineering. 2015;9(1).
[22] Abhale RB, Kandekar SB, Satpute MB. PVC confining effect on axially loaded column. Imperial J. Interdisciplinary Res. (IJIR). 2016; 2 (5):1391–1394.
[23] Kumutha R, Vijai K. External confinement of plain and reinforced concrete columns using PVC pipes. Proceedings of 2nd International Conference on Structural Architectural and Civil Engineering, 19th - 20th November 2016, in Dubai, U.A.E. p.72-78.
[24] Mammen AM, Antony M. Experimental study on FRP-PVC confined circular columns. International Research J Eng Techno. 2017; 04 (05): 1386-1390.
[25] Karthikeyan N, Akshatha B A, Sudhesh A S, Basavaraja N H. Assessment of Concrete Cylinders Confined with HDPE, PVC & UPVC Tubes. International Journal of Scientific & Engineering Research. 2018;9(4).
[26] Azeez A, Jamaluddin N, Abd Rahman N, Hassen D, Attiyah A. Experimental and Analytical study of PVC confined concrete cylinders. Journal of Engineering and Applied science. 2018;13(8):2145-2151.
[27] Woldemariam A, Oyawa W, Nyomboi T. Structural Performance of UPVC Confined Concrete Equivalent Cylinders Under Axial Compression Loads. Buildings. 2019;9:82. doi:10.3390/buildings9040082.
[28] Abdulla NA. A Strain model for uPVC tube-confined concrete. Cogent Eng. 2021;8(1):1868695. https://doi.org/10.1080/23311916.2020.1868695.
[29] Abdulla NA. Strength models for uPVC-confined concrete. Construction and Building Materials. 2021;310: 125070.
[30] Oberg E, Jones F. Machinery's Handbook, Revised and Enlarged. Industrial Press, 6th Edition. 1924.
[31] Yuan WB, Ma SL. Experimental Study on Concrete-Filled Steel Tubular with External Octagon Steel Tube and Inner Circle PVC-U Pipe under Axial Compression. Advanced Materials Research2012;368-373:511-514.